Algal Research 70 (2023) 102988

Contents lists available at ScienceDirect

Algal Research

journal homepage: www.elsevier.com/locate/algal

Complete N and P removal from hydroponic greenhouse wastewater by *Tetradesmus obliquus*: A strategy for algal bioremediation and cultivation in Nordic countries

João Salazar [a], Anita Santana-Sánchez [a], Juha Näkkilä [b], Sema Sirin [a,*], Yagut Allahverdiyeva [a,*]

[a] *Molecular Plant Biology, Department of Life Technologies, University of Turku, Turku FI-20014, Finland*
[b] *Natural Resources Institute Finland (Luke), Turku, Finland*

ARTICLE INFO

Keywords:
Greenhouse
Hydroponic
Photobioreactor
Microalgae
LED
Biomass characterization

ABSTRACT

Agricultural wastewaters are a major source of pollution in nature. Here, agricultural wastewaters from a commercial hydroponic greenhouse were used to cultivate the microalga *Tetradesmus obliquus* sp. NIVA-CHL107 in order to assess its bioremediation ability and evaluate the potential held in biomass derived from wastewater. The batch cultivation trials were performed using a pilot scale indoor photobioreactor equipped with LEDs. The culture achieved 100 % removal efficiency of N and P and a maximum dry weight (DW) of 6.2 g L^{-1}. At the exponential phase of growth, the biomass had a protein content of 45–50 % of DW and a carbohydrate fraction representing 20 % of DW. At the stationary phase, the carbohydrates increased to 60 % of DW. The PUFA content was higher during the exponential phase, representing >65 % of total fatty acids. Throughout the cultivation, the predominant carotenoids were lutein and β-carotene. The *Tetradesmus obliquus* sp. NIVA-CHL107 was demonstrated to be a suitable candidate for an algal biorefinery designed for hydroponic wastewater treatment and a multi-product pipeline.

1. Introduction

The transition towards a circular economy requires the use of waste streams as raw materials for a new generation of sustainable industries. One of the most promising sectors to develop this concept is the wastewater industry, as it holds significant potential for nutrient recovery and freshwater recycling. Worldwide, annual wastewater production is estimated to contain 16.6 Tg of N and 3.0 Tg of P [1]. On a smaller scale, at the European level, the wastewater network is estimated to hold an annual chemical recovery potential of 75 ktonnes of N and 67 ktonnes of P [2]. Each year, a significant portion of these waste streams is discharged directly to nature, resulting in severe impacts on the quality of habitats and ecosystems [3]. The most significant anthropogenic activity contributing to this unsustainable use of natural resources is agriculture, which currently represents 60 % of the total water use in the EU [4].

Agriculture is problematic in that mineral fertilizers and pesticides are used excessively and are thus unable to be efficiently taken up by crops. An increasingly significant portion of modern agriculture relies on indoor soilless cultivation strategies such as hydroponic systems to improve water management and maximize crop yields in order to effectively manage potential challenges posed by climate change [5,6]. In Europe and Canada, the greenhouse surface occupied by soilless cultivation systems is currently responsible for up to 95 % of the tomato production and in USA represents >90 % of cucumber production [7–9]. The European Hydroponics Market is predicted to grow rapidly with a revenue CAGR of 18.8 % during 2021–2027 [10]. Despite the progress in novel cultivation systems and plant nutrition, nutrient dosing in soilless farms is still far from optimal. Conventional hydroponic greenhouses are generally designed to operate in open or semi-closed systems and farmers avoid recirculating nutrient solutions to prevent salinity stress to the plants and to reduce the risk of contamination, which would compromise crop yield. This results in millions of liters of effluent being overloaded with nitrate and phosphate at the point of discharge [5,6,11]. Therefore, a transition towards a more sustainable agriculture sector represents a challenge that will require a continuous optimization of novel techniques, aiming for a reduction in the environmental footprint of the farms without compromising the yields and revenues of the farmers.

In the scope of a circular economy, a promising approach to deal

* Corresponding authors.
E-mail addresses: sesiri@utu.fi (S. Sirin), allahve@utu.fi (Y. Allahverdiyeva).

https://doi.org/10.1016/j.algal.2023.102988
Received 12 September 2022; Received in revised form 29 December 2022; Accepted 19 January 2023
Available online 24 January 2023

with hydroponic wastewaters lies in the recirculation of these waste streams for the cultivation of photosynthetic microorganisms [12,13]. Despite the higher concentrations of N and P in comparison with other types of wastewaters, several laboratory and pilot-scale experiments have already demonstrated the potential of microalgae and cyanobacteria in removing nutrients directly from hydroponic greenhouse effluents [14,15]. However, this approach is still at a conceptual stage due to several bottlenecks regarding: (i) the seasonal composition of the hydroponic wastewater which requires the need to constantly monitor and adjust the bioremediation process in order to efficiently purify these streams; (ii) the need to identify the most suitable strains and cultivation strategy to achieve maximum nutrient uptake and biomass production; (iii) the need to develop a valorization strategy for biomass derived from wastewaters.

In the present study, this bioremediation approach is evaluated as a strategy to purify hydroponic wastewater in Nordic countries. This study explores the concept of integrating microalgae production platforms into already existing greenhouse infrastructures. The indoor bioremediation proposed exploits the artificial light and temperature systems that are already deployed in Nordic agriculture to face geographic constraints and subarctic climates. This integrated strategy represents an opportunity to simultaneously purify the greenhouse wastewater and generate revenue through the produced algal biomass and its valorization. In our previous study, the identification of promising microalgae strain was achieved, however, the tubular photobioreactor (PBR) cultivation did not reach a satisfactory removal of nitrogen and failed to comply with the European directive for discharge of wastewater [15].

To this end, in the present study the microalga *Tetradesmus obliquus* sp. NIVA-CHL107 which was shown to outcompete several other genera of microalgae when cultivated in hydroponic wastewater at laboratory scale, was selected for a pilot scale cultivation in an indoor PBR using wastewater from a commercial hydroponic greenhouse [15]. Moreover, the PBR system was illuminated by a combination of natural sunlight and artificial light using red and blue LEDs in order to investigate if the addition of extra light would improve the removal efficiency of nitrogen. The experiments were performed in batch mode to evaluate the dynamics of nitrogen consumption, the most abundant nutrient in hydroponic wastewater, across the different stages of cell growth. Additionally, the biomass was biochemically characterized at exponential and stationary phases of the growth to determine the most suitable industrial applications.

2. Materials and methods

2.1. Experimental design

The microalga *Tetradesmus obliquus* sp. NIVA-CHL107 was cultivated in wastewater from a commercial hydroponic greenhouse. The two trials were performed in a tubular PBR equipped with red and blue LED lights commonly used in vegetable production greenhouses. The productivity and nutrient consumption of the culture were measured daily. Biomass was collected at exponential and stationary phases of growth to determine the biochemical composition regarding protein and carbohydrates as well as pigments and fatty acids (Fig. 1). The PBR was operated in batch mode and the trials were carried out in late October–November 2020 and March 2021 to evaluate repeatability of efficient removal of nitrogen and phosphorus considering the seasonal variation in natural sunlight and in the greenhouse wastewater.

2.2. Hydroponic greenhouse wastewater

For both trials the wastewater was obtained from a commercial hydroponic greenhouse (Puutarha Timo Juntti Oy) located in Kaarina, Finland and specialized in the production of cucumbers. The wastewater was collected prior to each trial and pretreated with a two-step filtration to remove solids and contaminants: (i) a coarse filtration (5 μm) and (ii) a membrane filtration using a 0.1 μm polyvinylidene fluoride (PVDF) membrane filter (Polymem, Waterpia GOLD, South Korea). After loading the PBR with the pretreated wastewater and inoculating the algae, a sample was collected to quantify the initial [N-NO_3^-], [P-PO_4^{3-}] and pH (Table 1). The wastewater from the hydroponic greenhouse had a nitrogen composition dominated by nitrate, with both N-NH_4^+ and N-NO_2^- concentrations being negligible. A detailed chemical composition of the wastewater can be found elsewhere [15].

Table 1
The macronutrient composition of hydroponic wastewater used in the present study.

	N-NO_3^- (mg L^{-1})	P-PO_4^{3-} (mg L^{-1})	N:P (molar ratio)	pH
Trial 1	284.8 ± 0.18	15.3 ± 0.01	41	6.9
Trial 2	235.0 ± 0.29	8.8 ± 0.04	59	7.7

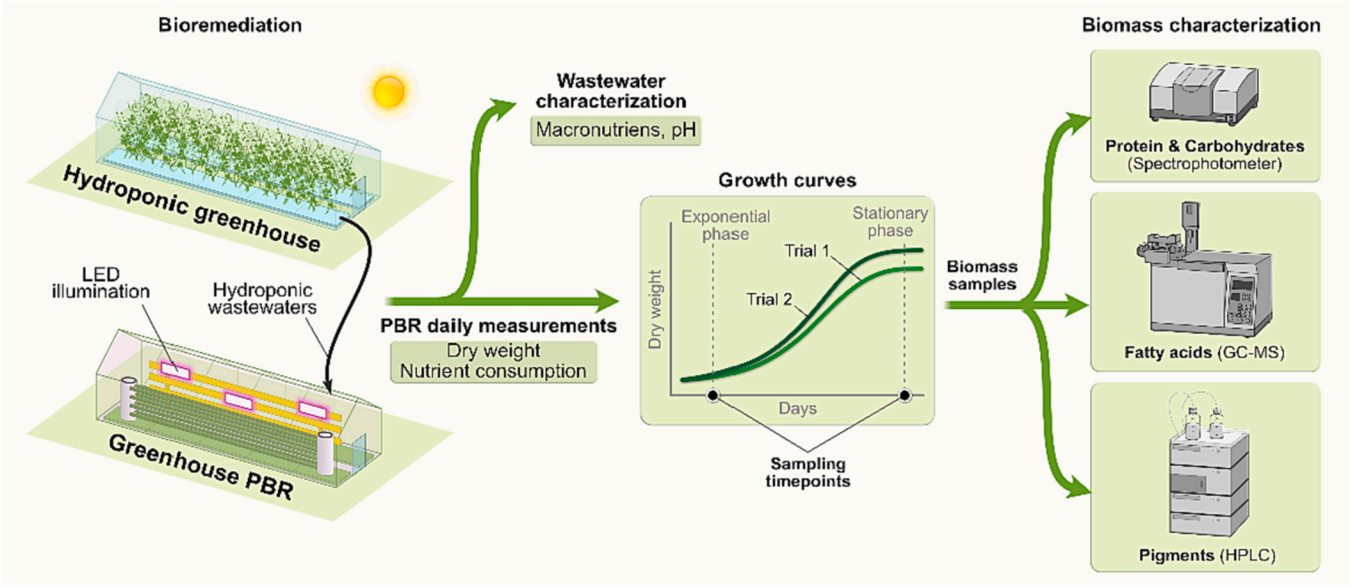

Fig. 1. The experimental design applied in the present manuscript. The biomass was freeze-dried and stored at −20 °C before the analytical characterization.

2.3. Microalga strain and inoculum

The *Tetradesmus obliquus* sp. NIVA-CHL107 (hereafter *Tetradesmus obliquus*) was obtained from the Norwegian Culture Collection of Algae (NORCCA). The strain was maintained in Z8 medium [16] under continuous low-intensity light (10 μmol m^{-2} s^{-1} photosynthetic photon flux density, PPFD) at room temperature (22 °C). For the PBR experiments, a 4 L inoculum was grown in BG11 medium (pH 7.5) in a glass bottle placed inside a growth chamber (Sanyo, Japan), providing a continuous light of 50 μmol m^{-2} s^{-1} PPFD at a constant temperature of 25 °C. The inoculum growth was undertaken in BG11 due to its similar [$N\text{-}NO_3^-$] composition with the hydroponic wastewater. The inoculum was mixed with a magnetic stirrer and sparged with filtered air +3 % CO_2. The culture growth was monitored until the late exponential phase by measuring OD_{750} (Genesys 10S UV–VIS, Thermo Fisher, USA).

2.4. PBR setup inside a greenhouse

A 65 L tubular PBR made of PLEXIGLAS-XT acrylic was assembled inside a glass greenhouse belonging to the Natural Resources Institute Finland (LUKE) and located in the Southwest-Finland region. The greenhouse is equipped with sustainable temperature control systems that rely on a biomass combustion furnace to produce energy and recirculate hot water. A detailed description of the tubular PBR system and greenhouse infrastructure can be found elsewhere [15,17]. Artificial light was provided throughout the algae cultivation period by five red and blue LED lights (200 W Overhead High Output, Netled Oy, Finland). The LED lights were evenly distributed on a wood frame and placed 1.3 m apart from one side of the PBR, in order to provide a homogeneous light distribution. The average intensity was approximately 320 μmol m^{-2} s^{-1} PPFD and a photoperiod of 17:7 h (light:dark) was applied following the conditions of cucumber cultivation. The glass greenhouse was equipped with a meteorological station which allowed real time monitoring of abiotic conditions such as temperature inside and outside, as well as solar radiation.

2.5. PBR operation and sample collection

Each trial was inoculated with a 4 L culture of *Tetradesmus obliquus* corresponding to an initial dry weight (DW) of approximately 0.2 g L^{-1}. A constant pH of 7.5 was set during cultivation which was controlled by automatic CO_2 injection. Samples were collected daily to assess the growth of the culture and the removal efficiency of nitrogen and phosphorus. A 1 L sample was collected in the beginning of the exponential phase (day 3) and all biomass was harvested at the end of the trial when the culture reached the stationary phase (day 20). The samples were centrifuged (Avanti J-20XP, Beckam Coulter, USA) and the pellets were quickly frozen in liquid nitrogen before freeze-drying (VirTis SP Scientific, USA).

2.6. Growth assessment

The culture growth was determined by means of DW (g L^{-1}). Samples were collected every day and 3 technical replicates were performed. The specific growth rate (d^{-1}), volumetric productivity (g L^{-1} d^{-1}) and areal productivity (g m^{-2} d^{-1}) were calculated as described in Salazar et al. [15] for batch mode PBR operation.

2.7. Nutrient consumption

Spectrophotometric methods were applied to determine the nutrient consumption and removal efficiencies of $N\text{-}NO_3^-$ and $P\text{-}PO_4^{3-}$. Calibration curves were prepared with $NaNO_3$ (>99 %, Merck) and K_2HPO_4 (99 %, VWR) using a spectrophotometer (Genesys 10S UV–VIS, Thermo Fisher, USA). Nitrate was quantified using the method 4500-NO3-B [18] and phosphate was determined using a test kit (Merck Spectroquant 1.14543). The daily samples were filtered through 0.45 μm Whatman syringe filters and diluted accordingly prior to analysis. Removal efficiencies (RE in %) for [$N\text{-}NO_3^-$] and [$P\text{-}PO_4^{3-}$] were calculated using 3 technical replicate measures according to Salazar et al. [15]. The nitrogen uptake (mg g^{-1} biomass d^{-1}) was calculated by dividing the daily [$N\text{-}NO_3^-$] consumption (mg N-NO3 L^{-1}) by the daily biomass accumulation (g L^{-1}) for each corresponding day.

2.8. Biomass characterization

2.8.1. Determination of protein

Protein content was determined according to the Lowry method [19]. A sample of 10 mg of freeze-dried biomass was suspended in a resuspension buffer as described in Zhang et al. [20]. Cell extraction was performed at 4 °C using a bead beater with 0.5 mm Zirconium Oxide beads for 5 min at maximum speed (Bullet Blender Storm 24, Next Advance, USA). The disrupted cell suspension was centrifuged at 15000 x*g* for a minute at 4 °C (Eppendorf, Germany) and the supernatant was collected for the protein assay. The extraction protocol was repeated 3 times for maximum recovery. The protein content in the supernatant was quantified using a kit (Bio-Rad DC Protein assay kit) and absorbance was measured at OD_{750}. Protein concentration was calculated from a bovine serum albumin (BSA) calibration curve ($R^2 = 0.998$). Sample extraction and analysis were performed in triplicate ($n = 3$).

2.8.2. Determination of carbohydrates

The content of carbohydrates was determined according to Dubois et al. [21]. Extraction was performed according to Alavijeh et al. [22] with minor modifications. A sample of 1 mg of freeze-dried biomass was resuspended in 0.5 mL of 2.5 M HCl and incubated in a dry heating block at 120 °C for 1 h (Grant Instruments, USA). Afterwards, samples were cooled down to room temperature and neutralized with 0.5 mL of 2.5 M NaOH. The mixture was centrifuged at 20000 ×*g* for 5 min and the supernatant was collected. In test tubes with screw caps, an aliquot of the supernatant was mixed with 5 % Phenol:H_2O (*v/v*) and 5 mL of H_2SO_4. The tubes were mixed by inversion and allowed to stand for 10 min before being transferred to a water bath where they were held at 30 °C for 15 min. A standard curve was prepared using glucose ($R^2 = 0.997$) and absorbance was measured at OD_{488}. Sample extraction and analyses were performed in triplicate ($n = 3$).

2.8.3. Determination of pigments

The cell extraction of pigments was performed by resuspending 5 mg of freeze-dried biomass in cold acetone. Samples were extracted using a bead beater as described earlier. Afterwards, the samples were centrifuged at 16000 ×*g* for 5 min and the supernatant was collected. The protocol was repeated 3 times for each sample to ensure maximum recovery. The supernatants were dried under a gentle stream of N_2, resuspended in methanol, and filtered into vials, using PTFE 0.2 μm pore size syringe filters. All steps were performed in a cold room under low light conditions.

The separation of pigments was performed following the protocol described in Kosourov et al. [23] using a HPLC equipped with a C18 Reverse Phase column (LiChrospher 100, 5 μm, Merck KGaA) and a diode array detector (Agilent 1100 series, Agilent technologies). A solvent gradient was used at a constant flow of 0.5 mL min^{-1}. Solvent A consisted of a mixture of acetonitrile/methanol/0.1 M Tris–HCl buffer adjusted to pH 8.0 (72:8:3) and solvent B consisted of methanol/hexane (4:1). Chromatographic peaks were identified by comparing retention times and spectra at OD_{440} against known standards (DHI, Denmark). Pigments were quantified using standard calibration curves. Sample extraction and analysis were performed in triplicate ($n = 3$).

2.8.4. Determination of fatty acid methyl ester

The fatty acid methyl ester (FAME) composition was determined according to Santana-Sánchez et al. [24] using a single-step extraction

and in situ transesterification as described in Wychen et al. [25]. Samples of 20 mg of freeze-dried biomass were resuspended using 200 μL of Chloroform: Methanol (2:1) and 300 μL of 0.6 M HCl:Methanol in 1.5 mL amber glass vials. The vials were gas-tight sealed and placed in a sand bath at 85 °C for an hour. After cooling down to room temperature, 1 mL of Hexane was added to separate the non-polar fraction. FAMEs were analyzed by GC–MS using an Agilent Innowax column (30 m × 0.32 mm, 19, 091 N-213, Agilent) with a film thickness of 0.5 μm and using Helium as the carrier gas. The column was programmed to maintain an initial temperature of 50 °C for 3 min and gradually increased at a rate of 15 °C per minute to a maximum of 250 °C, where it was held for 10 min. A standard FAME mix (C4:0-C24:0, Sigma Aldrich #18919-1AMP) was used to accurately identify individual FAMEs in the samples. The fatty acid methyl nonadecanoate (C19:0) was used as an internal standard. Sample peaks were identified based on retention times and validation was performed using software to compare the mass spectra (NIST MS Search 2.0). Sample extraction and analysis were performed in triplicate ($n = 3$).

2.9. Statistical analysis

The normality of the data was evaluated using the Shapiro-Wilk's test. The differences between the abiotic conditions (e.g. temperature, solar radiation) recorded during the PBR cultivation, as well as, the growth parameters in both trials were evaluated using a student's *t*-test. The homogeneity of variances of the data from the biochemical composition of the biomass was assessed using Levene's test. The significant differences in the biomass composition between different stages of the growth curve were investigated with a One-way ANOVA and confirmed using the Tukey HSD post-hoc test. All tests were performed with a significance level of $p = 0.05$ using the software IBM SPSS Statistics Version 27.

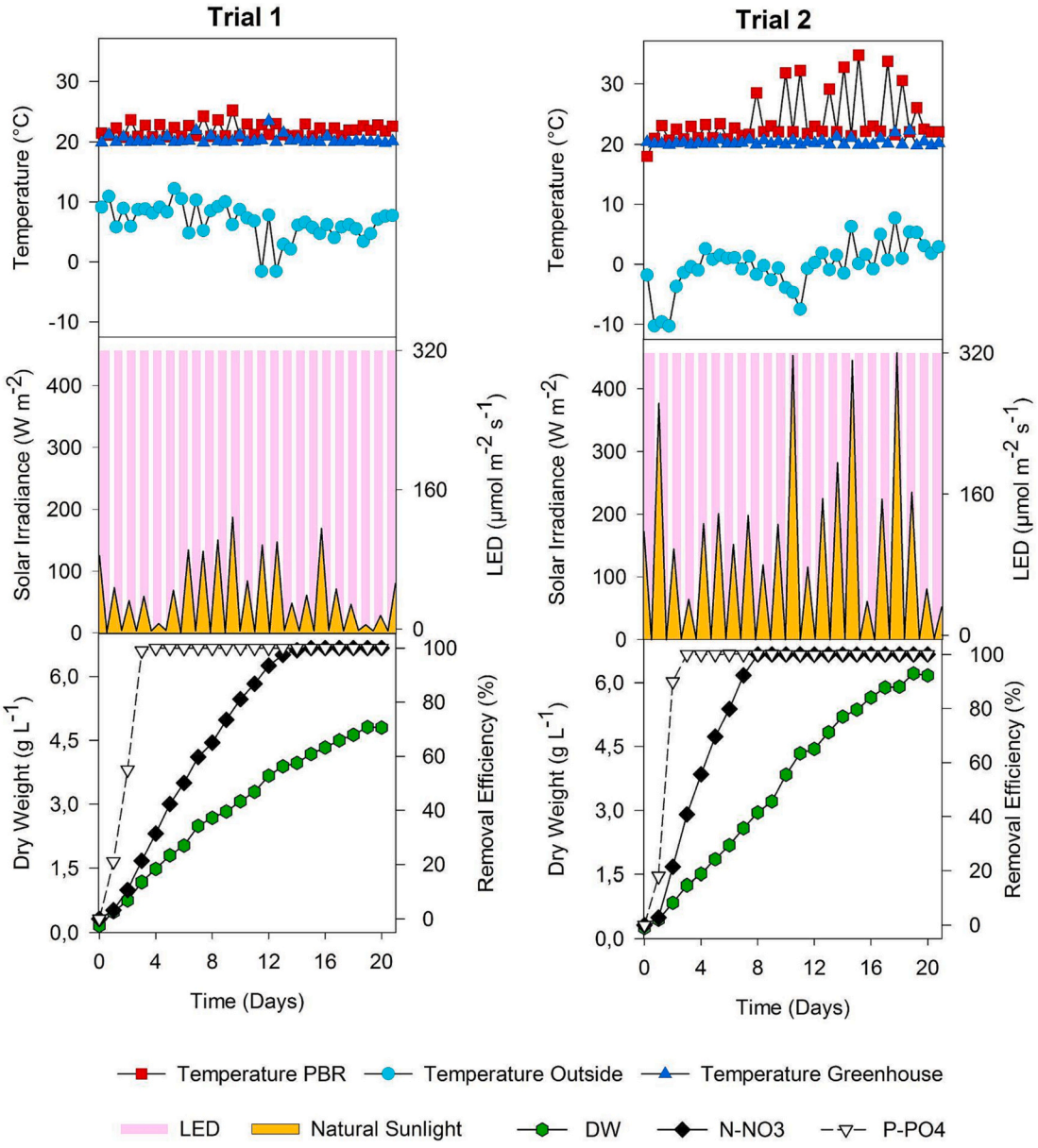

Fig. 2. Performance of the microalga *Tetradesmus obliquus* during the cultivation with hydroponic wastewater and respective abiotic conditions. Each data point for temperature and light corresponds to a 12-h period. The removal efficiency and dry weight data points are presented as mean ± standard deviation of technical replicates ($n = 3$). The maximum standard deviation for the removal efficiency was 0.8 % and for the dry weight was 0.15 g L^{-1}.

3. Results and discussion

3.1. Full removal of N and P in a PBR operating in batch mode in a greenhouse compartment

The microalga *Tetradesmus obliquus* was cultivated for 20 days in a greenhouse in a pilot scale PBR operated in batch mode under natural light and supplemental red and blue LED lights. In our previous lab-scale experiments we demonstrated that the *Tetradesmus* strain successfully proliferated in unadjusted hydroponic wastewater [15], therefore it was selected for pilot scale cultivation in an indoor PBR. Several other studies have shown that the genus *Tetradesmus* holds a potential to be an effective microbial bioremediation agent with the ability to adapt to different wastewaters [26–29]. In the current work, the bioremediation potential of this strain was assessed by using unadjusted hydroponic wastewater as growth media and monitoring the dynamics of nitrogen removal during different phases of cell growth. Two trials were performed at the beginning and end of the cold season in Finland (November and March) to evaluate the feasibility of combining a greenhouse infrastructure and artificial light with an algal cultivation system for pilot-scale bioremediation purposes. During November the daily photoperiod of natural sunlight is reduced to <8 h, while in March it reaches almost 12 h. The abiotic conditions, growth performance and nutrient removal efficiency achieved during the cultivation of the microalga *Tetradesmus obliquus* are shown in Fig. 2. The trials demonstrated the suitability of the unadjusted hydroponic wastewater as a productive growth media for *Tetradesmus obliquus* despite the high N:P ratios (Table 1).

Trial 1 was performed during late October and throughout November 2020 (Fig. 2). During this period, the temperatures outside the greenhouse oscillated between −1.6 °C and 12.2 °C with an average temperature of 6.7 ± 2.9 °C. The greenhouse infrastructure kept the temperature inside the PBR constant at 22.0 ± 1.1 °C. The maximum temperature during Trial 1 was 25.2 °C with the highest solar radiation recorded for this period. In Finland, solar radiation drastically decreases during the winter season not only in regards to intensity, but also to the total daily hours of sunlight. During Trial 1, the maximum solar radiation was 187 W m^{-2} and the average photoperiod for natural sunlight was 7.7 ± 0.5 h day^{-1}. The greenhouse wastewater had an initial [N-NO_3^-] of 284.84 ± 0.18 mg L^{-1} and [P-PO_4^{3-}] of 15.33 ± 0.01 g L^{-1}. Under this set of conditions, no lag phase was observed after inoculation. At day 3 of cultivation, the culture had accumulated a DW of 1.12 ± 0.04 g L^{-1} and achieved 100 % removal efficiency for P-PO_4^{3-}. From this point on, the culture continued to grow without any additional P-PO_4^{3-}, which indicates a cellular strategy of luxury uptake and storage [29].

On day 13, the culture was able to remove 97.5 % of N-NO_3^- which met the total N discharge criteria of the EU directive concerning urban wastewater treatment (91/271/EEC). The culture achieved 100 % removal efficiency of N-NO_3^- at day 15 and continued to grow until the end of the trial (day 20) accumulating a maximum DW of 4.8 ± 0.02 g L^{-1}.

Trial 2 was conducted during March 2021 (Fig. 2). During this cultivation period, the minimum temperature recorded outside the greenhouse was −10.3 °C and the average temperature inside the PBR was 24.0 ± 4.1 °C. The highest recorded solar radiation was 457 W m^{-2} and the average photoperiod for natural sunlight was 11.9 ± 0.55 h day^{-1}. There was a significant difference in the average temperatures inside the PBR between Trials 1 and 2, which was likely a direct consequence of the increase in the total amount of solar radiation and photoperiod. During Trial 2, the culture received approximately 4 more hours of natural sunlight each day in comparison to Trial 1.

The greenhouse wastewater had an initial [N-NO_3^-] of 235.02 ± 0.29 mg L^{-1} and [P-PO_4^{3-}] of 8.79 ± 0.04 mg L^{-1} and after inoculation of the culture in the PBR, similarly to Trial 1, no lag phase was recorded. At day 3 of cultivation, the culture had accumulated a DW of 1.25 ± 0.02 g L^{-1} and achieved 100 % removal efficiency of P-PO_4^{3-}. During the following days the culture continued to grow, achieving 100 % removal efficiency of N-NO_3^- at day 8 of cultivation and meeting the criteria of the EU directive (91/271/EEC) seven days earlier than in Trial 1. From this point onwards, the culture continued to grow until the stationary phase (day 20) and accumulated a maximum DW of 6.2 ± 0.03 g L^{-1}.

At the end of Trial 2, the biomass accumulation was higher than in Trial 1 even though the initial concentrations of nitrogen and phosphorus in the wastewater were lower (Table 1). This outcome can be explained by a more favorable setup of abiotic conditions, which allowed the culture in Trial 2 to increase its nitrogen removal by almost 2-fold in comparison to Trial 1, particularly during the early stages of exponential growth (Figs. 2, 3). For both trials, biomass accumulation was similar until day 8, however in Trial 1 the culture achieved a maximum nitrogen uptake of 97.84 ± 4.76 mg g^{-1} d^{-1} which is significantly lower in comparison with the maximum nitrogen uptake of Trial 2 (132.54 ± 14.02 mg g^{-1} d^{-1}, Fig. 3). The maximum nitrogen uptake corresponded to a cell DW of ~1.5 g L^{-1} for both trials. The results in Trial 2 also surpassed our previous experiments regarding nitrogen uptake; however, it is important to mention that in the present manuscript a different species and light system were tested [15]. For Trial 2, it is also worth mentioning that despite the constant temperatures inside the PBR at the early stages of cultivation (until day 8 when 100 % removal efficiency of N-NO_3^- was achieved), there was a substantial increase in the total amount of sunlight (Fig. 2). This outcome suggests that light, not temperature, is most likely the main factor affecting nitrogen uptake. At the early stages of exponential growth, the low biomass concentrations inside the PBR allowed for a higher light penetration of solar radiation and LEDs, which combined with a scenario of nutrient replete conditions resulted in a maximum nitrogen uptake (Fig. 3) [30].

The specific growth rates and productivities of *Tetradesmus obliquus* for both trials are shown in Table 2. The results demonstrate a better performance of the culture during Trial 2 when the overall solar radiation was significantly higher. The specific growth rates of *Tetradesmus obliquus* were 0.13 ± 0.002 d^{-1} and 0.15 ± 0.002 d^{-1} in Trial 1 and Trial 2 respectively. Similar growth rates have been described for other strains of *Tetradesmus* sp. cultivated in wastewater streams [31]. However, the biomass concentration in the present study substantially exceeded previously reported numbers for closed batch PBR cultivation [32–34]. This result might be a consequence of the interaction between different factors: (i) nutrient composition of the wastewater; (ii) the greenhouse environment; (iii) the supplementary red and blue LED illumination and its light path length. In fact, the use of LED lights with single or multiple wavelengths for the cultivation of *Tetradesmus* species in tubular PBR has been previously reported, suggesting benefits regarding biomass productivity when the cultures are exposed to white: green, single blue or red:blue wavelengths [35]. The same trend has also been observed for lab scale cultivation of *Tetradesmus* species [36]. Nonetheless, the distance between the light source and the PBR has also been described to contribute greatly to the maximum cell density inside any given cultivation system [37]. Therefore, this outcome results from a complex matrix of factors that deserves further study.

In the present study, the use of artificial light ensured a steady supply of photons for both trials and lessened to some extent the effects of fluctuating natural photoperiod. However, it is worth mentioning that the high concentration of cells inside the PBR is known to significantly affect the penetration of certain wavelengths, therefore the individual contribution of natural light, red and blue photons to the nitrogen uptake rate and conversion into biomass accumulation deserves to be further explored [38]. This aspect is particularly relevant for Nordic countries which rely on artificial light to produce algal biomass. Overall, the benefits and limitations of using artificial light in microalgae cultivation systems have been widely discussed, with several pilot-scale studies suggesting the feasibility of applying LEDs when algal biomass is targeted for high-value products [39]. The use of LED illumination with single or multiple wavelengths has been linked to metabolic

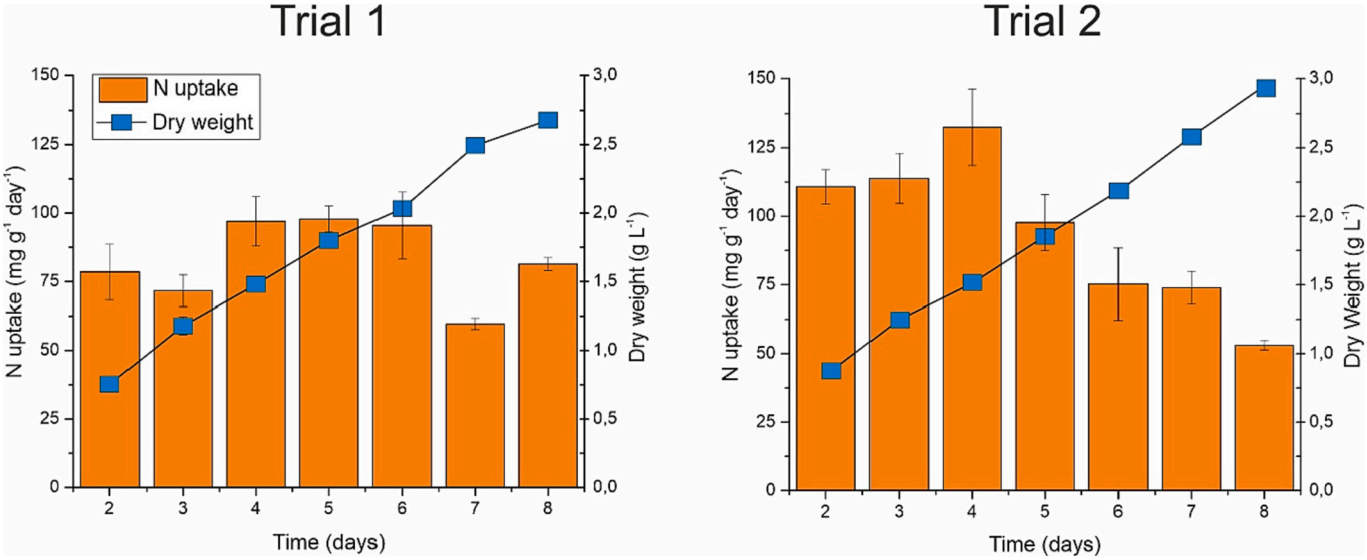

Fig. 3. The daily dynamics of nitrogen uptake for the microalgae *Tetradesmus obliquus* cultivated in an indoor PBR illuminated by natural sunlight and red and blue LEDs. Data is presented as mean ± standard deviation of technical replicates ($n = 3$). The maximum standard deviation of the dry weight is 0.05 g L^{-1}. (For interpretation of the references to colour in this figure legend, the reader is referred to the web version of this article.)

Table 2
The specific growth rate and biomass productivities of *Tetradesmus obliquus*. Data is presented as mean ± standard deviation ($n = 3$) considering the time interval of the exponential phase of growth (days 1 to 19). Different upper letters in the same column represent statistically significant differences between each sample group.

	Specific growth rate (d^{-1})	Volumetric Productivity (g L^{-1} d^{-1})	Areal Productivity (g $m^{-2}d^{-1}$)
Trial 1	0.13 ± 0.002[a]	0.24 ± 0.002[a]	15.15 ± 0.129[a]
Trial 2	0.15 ± 0.002[b]	0.32 ± 0.002[b]	20.19 ± 0.139[b]

changes in several genera of microalgae which resulted in improved nutrient uptake rates as well as different biochemical composition of the biomass [40].

3.2. Composition of the biomass produced in hydroponic wastewater

The biochemical characterization of biomass was performed for samples collected at the exponential and stationary phases of growth. The biomass composition was determined regarding protein and carbohydrate content, as well as fatty acids and pigments. These molecular groups were qualitative and quantitatively analyzed to evaluate the potential value of the biomass for possible industrial applications.

3.2.1. Protein and carbohydrates

The biomass from the exponential phase of Trial 1 had a protein content of 44.6 ± 1.8 % of DW and a carbohydrate content of 20.5 ± 0.8 % of DW (Fig. 4). In Trial 2, the biomass of the exponential phase had a similar carbohydrate content (21.4 ± 0.6 % of DW), however the protein content was significantly higher (52.8 ± 1.9 % of DW). This outcome can be a direct consequence of the higher N uptake observed in the early stages of the cultivation which combined with a better set of abiotic conditions led to an increase in protein synthesis (Figs. 2 and 3). At the stationary phase of growth, the biomass from both trials presented a

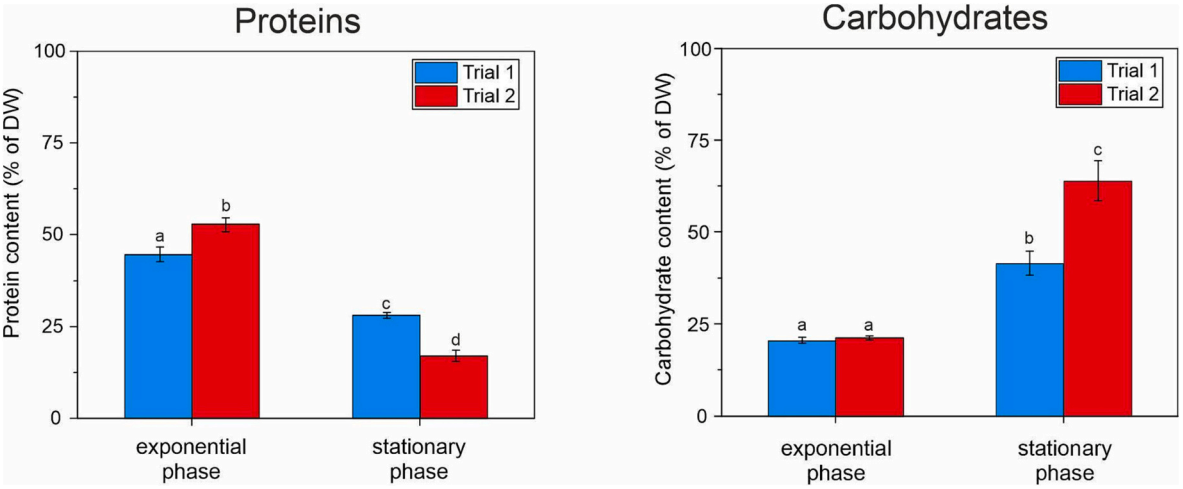

Fig. 4. The content of protein and carbohydrates in *Tetradesmus obliquus* biomass harvested at different stages of growth. Data is presented as the mean ± standard deviation of technical replicates ($n = 3$). Different letters represent statistically significant differences at different stages of growth.

substantial lower content of protein and a significantly higher concentration of carbohydrates (Fig. 4).

During Trial 1, the biomass from the stationary phase had a protein content of 28.1 ± 0.8 % of DW and the carbohydrate fraction represented 41.7 ± 3.3 % of DW. Likewise, at the end of the Trial 2, the biomass presented a protein content of 17.0 ± 1.5 % of DW while the carbohydrate fraction achieved its maximum value of 63.9 ± 5.4 % of DW.

The results confirm that protein concentration at different stages of growth is strongly affected by nitrogen availability. Nitrogen replete conditions during the early stages of growth promoted an allocation of C and N towards protein synthesis, whereas, at later stages of cultivation, the metabolism of the N depleted cells shifted towards carbohydrate accumulation. In the exponential phase of growth, the culture had a protein:carbohydrate molecular ratio of 2.17 and 2.47 for Trial 1 and Trial 2, respectively. At the stationary phase of growth, the molecular ratios decreased significantly to 0.68 and 0.27 for Trial 1 and Trial 2, which was a direct consequence of the nutrient depletion. A similar metabolic behavior has also been reported for other species of the *Tetradesmus* genus [38]. Nonetheless, in the presence of N and P in the growth medium, it is also possible for *Tetradesmus obliquus* to accumulate higher amounts of protein in comparison with carbohydrates during the stationary phase of growth [26,41].

3.2.2. Pigment composition

The pigment composition of the biomass at the exponential and stationary phases of growth is presented in Table 3. The total amount of chlorophyll was significantly higher at the exponential phase of growth in comparison with the stationary phase. During the exponential phase of growth there were no statistically significant differences in the amount of the primary pigments, chlorophyll *a* and *b*, between both trials (Table 3).

This suggests a relationship between high cell division and the need for efficient photosynthesis as a direct supply of energy. However, a different trend was observed at the stationary phase, where the amounts of chlorophyll *a* and *b* were significantly different between both trials (Table 3). In the stationary phase of Trial 2, the low content of primary pigments may have resulted from the combined effect of the increased solar radiation and the prolonged nutrient deprivation leading to photoinhibition [42].

For both trials, the highest amounts of carotenoids were observed at the exponential phase of growth (Table 3). During this stage, light penetration inside the PBR was higher due to a lower cell concentration, which might have induced photodamage and upregulated carotenoid production as a photoprotection mechanism. Across all growth phases, the most abundant carotenoid in the biomass was lutein, followed by *β*-carotene. A similar trend was observed at laboratory scale using *Scenedesmus obliquus* [43]. In the course of Trial 1, there were no significant differences in the concentrations of lutein (Table 3). In Trial 2, the maximum amount of lutein was recorded during the exponential phase of growth, at 3.03 ± 0.11 mg g^{-1} of DW biomass. This maximum value is slightly higher than that reported in *Tetradesmus obliquus* [44] however it is approximately 10-fold lower than the one reported in *Scenedesmus obliquus* [43]. The same result was observed for violaxanthin with the present study registering the lowest value of 0.34 ± 0.05 mg g^{-1} during the stationary phase and the highest amount of 1.02 ± 0.05 mg g^{-1} at the exponential phase of Trial 2.

In both trials, the concentrations of the carotenoid *β*-carotene were higher during the exponential phase of growth (Table 3). In Trial 1, the maximum value was 0.90 ± 0.10 mg g^{-1} which is not significantly different from the 1.29 ± 0.32 mg g^{-1} achieved in Trial 2. These values are in agreement with literature [45].

Table 3
Pigment composition of *Tetradesmus obliquus* at exponential and stationary phases of growth. Data represents the mean ± standard deviation of technical replicates ($n = 3$). Different upper letters in the same row represent statistically significant differences between each sample group.

Pigments (mg g^{-1} DW)	T1 Exponential	T1 Stationary	T2 Exponential	T2 Stationary
Chlorophyll *a*	47.25 ± 7.18^{a}	30.67 ± 3.23^{b}	50.71 ± 1.44^{a}	14.74 ± 1.09^{c}
Chlorophyll *b*	6.76 ± 1.72^{a}	3.65 ± 0.67^{b}	6.51 ± 0.26^{a,b}	0.51 ± 0.19^{c}
Violaxanthin	0.74 ± 0.03^{a}	0.53 ± 0.08^{b}	1.02 ± 0.05^{c}	0.34 ± 0.05^{d}
Lutein	2.47 ± 0.13^{a,b}	2.49 ± 0.40^{a,b}	3.03 ± 0.11^{a}	1.93 ± 0.24^{b}
α-Carotene	0.47 ± 0.06^{a}	0.24 ± 0.03^{b}	0.67 ± 0.06^{c}	n.d.
β-Carotene	0.90 ± 0.10^{a,b}	0.78 ± 0.07^{a,b}	1.29 ± 0.32^{a}	0.47 ± 0.04^{b}

3.2.3. FAME composition

The fatty acid composition of the biomass at exponential and stationary phases of growth is presented in Table 4. For both trials and across all stages of the growth, the results demonstrate that the FAME composition of *Tetradesmus obliquus* contained high levels of polyunsaturated fatty acids (PUFAs), a moderate amount of saturated fatty acids (SFAs) and a low content of monounsaturated fatty acids (MUFAs). In the course of Trial 1, there was no significant difference in the relative abundance of SFAs between exponential and stationary phases. In the exponential phase of Trial 2, the presence of SFA represented 19.80 ± 0.30 % of the total fatty acid (TFA) content which was significantly lower than the stationary phase (26.70 ± 0.25 % of TFA).

In both trials, the most abundant SFA was the palmitic acid (C16:0) ranging from 18 to 24 % of TFA, while myristic (C14:0), stearic (C18:0) and behenic (C22:0) acids were only present in residual amounts.

The MUFA fraction in both trials was mainly represented by palmitoleic (C16:1, ω-7) and oleic (C18:1, ω-9) acids while the 11-eicosenoic acid also known as gondoic acid (C20:1, ω-9) was only detected in residual amounts at the stationary phase of growth. In both trials the MUFA fraction was significantly higher at the stationary phase of growth. Although the percentages of each fatty acid can vary greatly

Table 4
The FAME composition of the biomass (% of total fatty acids) for *Tetradesmus obliquus* at different stages of growth. Data represents the mean ± standard deviation of technical replicates ($n = 3$). Different upper letters in the same row represent statistically significant differences between each sample group.

FAME (% of total FA)	T1 Exponential	T1 Stationary	T2 Exponential	T2 Stationary
C 14:0	0.53 ± 0.04^{a}	0.61 ± 0.04^{a}	0.51 ± 0.03^{a}	0.57 ± 0.01^{a}
C 16:0	21.28 ± 3.64^{a,b}	19.90 ± 1.64^{a,b}	17.66 ± 0.24^{a}	24.17 ± 0.11^{b}
C 18:0	0.73 ± 0.02^{a}	0.71 ± 0.06^{a}	0.71 ± 0.01^{a}	1.14 ± 0.02^{b}
C 22:0	0.90 ± 0.03^{a}	0.96 ± 0.19^{a}	0.92 ± 0.01^{a}	0.82 ± 0.11^{a}
Σ SFA	23.44 ± 3.73^{a,b}	22.18 ± 1.94^{a,b}	19.80 ± 0.30^{a}	26.70 ± 0.25^{b}
C 16:1 (ω-7)	4.03 ± 0.12^{a}	4.14 ± 0.29^{a}	4.41 ± 0.1^{a}	3.51 ± 0.13^{b}
C 18:1 (ω-9)	4.11 ± 0.23^{a}	6.17 ± 0.38^{b}	2.60 ± 0.05^{c}	12.52 ± 0.87^{d}
C 20:1	n.d.	0.82 ± 0.12^{a}	n.d.	0.90 ± 0.07^{a}
Σ MUFA	8.14 ± 0.35^{a}	11.12 ± 0.79^{b}	7.02 ± 0.15^{a}	16.93 ± 1.06^{c}
C 16:2	0.71 ± 0.03^{a}	0.82 ± 0.06^{b}	0.64 ± 0.01^{a}	1.12 ± 0.02^{c}
C 16:3 (ω-3)	3.22 ± 0.20^{a,b}	2.59 ± 0.08^{b}	2.95 ± 0.18^{a,b}	3.64 ± 0.02^{a}
C 16:3 (ω-6)	1.09 ± 0.03^{a}	1.12 ± 0.12^{a}	1.00 ± 0.02^{a,b}	0.86 ± 0.05^{b}
C 16:4 (ω-3)	19.41 ± 0.95^{a}	16.33 ± 0.13^{b}	20.03 ± 0.4^{a}	11.31 ± 0.01^{c}
C 18:2 (ω-6)	4.90 ± 0.22^{a}	7.81 ± 0.06^{b}	3.97 ± 0.08^{c}	7.60 ± 0.06^{b}
C 18:3 (ω-3)	36.67 ± 1.80^{a}	30.68 ± 0.71^{b}	41.67 ± 0.78^{c}	25.85 ± 0.32^{d}
C 18:3 (ω-6)	n.d.	1.50 ± 0.05^{a}	n.d.	0.98 ± 0.02^{b}
C 18:4 (ω-3)	2.43 ± 0.05^{a}	5.85 ± 0.27^{b}	2.92 ± 0.1^{c}	5.01 ± 0.06^{d}
Σ PUFA	68.42 ± 3.29^{a,b}	66.70 ± 1.50^{a}	73.18 ± 1.58^{b}	56.37 ± 05.7^{c}

with the experimental design, the composition of SFAs and MUFAs reported in the present study are similar to literature [46,47]. Across all stages of the cultivation, the PUFAs were the most abundant fatty acids in the biomass ranging from 56 to 73 % TFA. In both trials, the main PUFAs were the α-linolenic acid (C18:3, ω-3) and the 4,7,10,13 hexadecatetraenoic acid (C16:4, ω-3). The linoleic (C 18:2, ω-6) and stearidonic (C 18:4, ω-3) acids were detected in moderate amounts varying from 2 to 8 % of TFA. A similar PUFA content has been reported for a *Tetradesmus wisconsinensis* cultivation illuminated with white LEDs [47].

In the present study, the residual amounts of C18:0 across all stages of the cultivation suggest that this fatty acid can be the main precursor of the PUFA synthesis in this strain [48]. Although it has been proposed that microalgae tend to accumulate more PUFAs in low temperature conditions, our results show that PUFAs were the main fraction of the FAMEs even when temperatures inside the PBR were between 22 and 24 °C [49]. This outcome might be explained by the depletion of P-PO_4^{3-} registered from day 3 onwards which has been observed to be a factor significantly contributing for the synthesis of PUFAs in *Tetradesmus obliquus* cultures [50].

These metabolic responses to nutrient availability can be controlled if nutrient consumption is monitored regularly to prevent depletion. The addition of nutrients during cultivation to prevent cellular stress has been studied at industrial scale as a method to produce biomass with a balanced chemical composition throughout all stages of growth [51]. Taken together, these results suggest that the feasibility of scaling-up bioremediation projects using microalgae is strongly linked to the N and P composition of the waste streams as well as the cultivation setup, as it will drastically affect the composition and the applications of the resulting biomass.

3.2.4. Future perspectives on microalgae bioremediation of hydroponic wastewaters

In both trials, the batch cultivation of *Tetradesmus obliquus* resulted in 100 % removal efficiency of N and P from hydroponic wastewaters. The maximum N uptake of the cultures occurred at the early exponential phase of growth which is characterized for being a period of high cell division, biomass growth and volumetric productivity. This outcome supports the idea that *Tetradesmus obliquus* is a promising strain for bioremediation of hydroponic wastewaters, due to the possibility of operating a continuous cultivation system with a short hydraulic retention time that would allow to purify a significant portion of nutrient rich wastewaters in a short period of time.

As the PBR used in the present study can also be operated in continuous mode, it is worth mentioning that in the future it is possible to establish a DW threshold corresponding to the cellular stage of maximum nutrient uptake rate. In this case, the biomass of *Tetradesmus obliquus* is expected to contain high amounts of protein, pigments and PUFAs, which will be of great interest for the formulation of aquaculture, cattle and poultry feeds, or the agriculture sector in the form of plant biostimulants and biopesticides for crops [52,53].

The microalgae biomass produced from wastewaters is often excluded from animal feed applications because of the hazardous substances present in the streams during cultivation. Despite the constant need to monitor the presence of compounds such as pesticides, hydroponic wastewater solutions are already regulated under the EU - Fertilizing Products Regulation, ensuring safety of use for vegetable production and human consumption [54]. Therefore, the use of hydroponic wastewaters can represent an opportunity to use microalgae biomass in these markets and accelerate circular economy business models. In the scope of this concept, a downstream pipeline should be developed to separate all relevant fractions and increase the profitability of the biomass. In that case, the use of non-toxic waste streams, such as hydroponic effluents as growth media for photosynthetic microorganisms can promote the deployment of a new generation of sustainable industries.

4. Conclusion

The cultivation of *Tetradesmus obliquus* in a photobioreactor equipped with LEDs and assembled inside a greenhouse, proved to be an efficient strategy for bioremediation of hydroponic effluent. The microalga *Tetradesmus obliquus* proliferated in unadjusted effluent achieving 100 % removal of N and P. The biomass derived from hydroponic effluent displayed a chemical composition comparable to that of traditional growth media and can be used for several industrial applications. The biomass composition is dependent on the growth phase which can have a significant impact on its application and allows for a tunable product on the basis of market needs.

Funding

This research was financially supported by the NordForsk Nordic Center of Excellence 'NordAqua' (project #82845 to YA).

CRediT authorship contribution statement

João Salazar: Conceptualization, Data curation, Formal analysis, Investigation, Methodology, Writing – original draft. **Anita Santana-Sánchez:** Investigation, Methodology. **Juha Näkkilä:** Resources. **Sema Sirin:** Conceptualization, Data curation, Methodology, Validation, Supervision, Writing – review & editing. **Yagut Allahverdiyeva:** Conceptualization, Funding acquisition, Project administration, Supervision, Writing – review & editing.

Declaration of competing interest

The authors declare that they have no known competing financial interests or personal relationships that could have appeared to influence the work reported in this paper.

Data availability

Data will be made available on request.

Acknowledgements

The authors would like to thank NordAqua partner organization NIVA (Norway) for sharing the microalga strain of *Tetradesmus obliquus* from the Norwegian Culture Collection of Algae (NORCCA) and "Puutarha Timo Juntti Oy" greenhouse for providing the hydroponic wastewater. The authors express their gratitude to the staff at LUKE's research greenhouse for the LED setup for the PBR cultivation, as well as, to Tapio Ronkainen (UTU, Finland) for the technical support and to Dr. Fiona Lynch for critically reading the manuscript. The authors would also like to thank Dr. Dmitry Shevela (ShevelaDesign AB, Sweden) for the illustration of the graphic abstract and Fig. 1.

References

[1] M. Qadir, P. Drechsel, B. Jiménez Cisneros, Y. Kim, A. Pramanik, P. Mehta, O. Olaniyan, Global and regional potential of wastewater as a water, nutrient and energy source, Nat. Res. Forum 44 (2020) 40–51, https://doi.org/10.1111/1477-8947.12187.
[2] EurEau - The European Federation of National Associations of Water Services, Factsheet on Products From Waste Water - Minerals, 2021.
[3] HELCOM, Input of Nutrients by the Seven Biggest Rivers in the Baltic Sea Region 1995-2017, HELCOM, 2021.
[4] EEA- European Environment Agency, Water And Agriculture: Towards Sustainable Solutions, 2021.
[5] D. Savvas, N. Gruda, Application of soilless culture technologies in the modern greenhouse industry – a review, Eur. J. Hortic. Sci. 83 (2018) 280–293, https://doi.org/10.17660/eJHS.2018/83.5.2.
[6] G. Samiotis, C. Lykas, I. Ristanis, A.Z. Stimoniaris, E. Amanatidou, Integrated management of hydroponic wastewater for complete water recycle and cyanobacteria cultivation using an electric conductivity-based tool, Bioresour. Technol. Rep. (2022), 101191, https://doi.org/10.1016/j.biteb.2022.101191.

[7] N.S. Gruda, Increasing sustainability of growing media constituents and stand-alone substrates in soilless culture systems, Agronomy 9 (2019) 298, https://doi.org/10.3390/agronomy9060298.

[8] L. Incrocci, R.B. Thompson, M.D. Fernandez-Fernandez, S. De Pascale, A. Pardossi, C. Stanghellini, Y. Rouphael, M. Gallardo, Irrigation management of European greenhouse vegetable crops, Agric. Water Manag. 242 (2020), 106393, https://doi.org/10.1016/j.agwat.2020.106393.

[9] K.J. Walters, B.K. Behe, C.J. Currey, R.G. Lopez, Historical,current, and future perspectives for controlled environment hydroponic food crop production in the United States, Horts 55 (2020) 758–767, https://doi.org/10.21273/HORTSCI14901-20.

[10] KBV, Europe hydroponics market size, share & industry trends analysis report by type, by crops (tomatoes, lettuce, peppers, cucumbers, herbs, fruits, and others), by country and growth forecast, 2021 - 2027. https://www.kbvresearch.com/europe-hydroponics-market/, 2022.

[11] P. Sambo, C. Nicoletto, A. Giro, Y. Pii, F. Valentinuzzi, T. Mimmo, P. Lugli, G. Orzes, F. Mazzetto, S. Astolfi, R. Terzano, S. Cesco, Hydroponic solutions for soilless production systems: issues and opportunities in a smart agriculture perspective, Front. Plant Sci. 10 (2019) 923, https://doi.org/10.3389/fpls.2019.00923.

[12] R. Díez-Montero, V. Belohlav, A. Ortiz, E. Uggetti, M.J. García-Galán, J. García, Evaluation of daily and seasonal variations in a semi-closed photobioreactor for microalgae-based bioremediation of agricultural runoff at full-scale, Algal Res. 47 (2020), 101859, https://doi.org/10.1016/j.algal.2020.101859.

[13] P.C. Gorain, I. Paul, P.S. Bhadoria, R. Pal, An integrated approach towards agricultural wastewater remediation with fatty acid production by two cyanobacteria in bubble column photobioreactors, Algal Res. 42 (2019), 101594, https://doi.org/10.1016/j.algal.2019.101594.

[14] F. Delrue, P. Álvarez-Díaz, S. Fon-Sing, G. Fleury, J.-F. Sassi, The environmental biorefinery: using microalgae to remediate wastewater, a win-win paradigm, Energies 9 (2016) 132, https://doi.org/10.3390/en9030132.

[15] J. Salazar, D. Valev, J. Näkkilä, E. Tyystjärvi, S. Sirin, Y. Allahverdiyeva, Nutrient removal from hydroponic effluent by Nordic microalgae: from screening to a greenhouse photobioreactor operation, Algal Res. 55 (2021), 102247, https://doi.org/10.1016/j.algal.2021.102247.

[16] J. Kotai, Instructions for Preparation of Modified Nutrient Solution Z8 for Algae, 1972.

[17] D. Valev, H. Silva Santos, E. Tyystjärvi, Stable wastewater treatment with Neochloris oleoabundans in a tubular photobioreactor, J. Appl. Phycol. 32 (2020) 399–410, https://doi.org/10.1007/s10811-019-01890-x.

[18] APHA Method 4500-NO3: Standard Methods for the Examination of Water and Wastewater, (n.d.) 12.

[19] Oliver H. Lowry, Nira J. Rosebrough, A.L. Farr, Rose J. Randall, Protein measurements with the folin phenol reagent, J.Biol.Chem. (1951), https://doi.org/10.1016/S0021-9258(19)52451-6.

[20] P. Zhang, Y. Allahverdiyeva, M. Eisenhut, E.-M. Aro, Flavodiiron proteins in oxygenic photosynthetic organisms: photoprotection of photosystem II by Flv2 and Flv4 in Synechocystis sp. PCC 6803, PLoS ONE 4 (2009), e5331, https://doi.org/10.1371/journal.pone.0005331.

[21] Michel DuBois, K.A. Gilles, J.K. Hamilton, P.A. Rebers, Fred Smith, Colorimetric method for determination of sugars and related substances, Anal. Chem. 28 (1956) 350–356, https://doi.org/10.1021/ac60111a017.

[22] R.S. Alavijeh, K. Karimi, R.H. Wijffels, C. van den Berg, M. Eppink, Combined bead milling and enzymatic hydrolysis for efficient fractionation of lipids, proteins, and carbohydrates of Chlorella vulgaris microalgae, Bioresour. Technol. 309 (2020), 123321, https://doi.org/10.1016/j.biortech.2020.123321.

[23] S. Kosourov, G. Murukesan, J. Jokela, Y. Allahverdiyeva, Carotenoid biosynthesis in Calothrix sp. 336/3: composition of carotenoids on full medium, during diazotrophic growth and after long-term H 2 photoproduction, Plant Cell Physiol. 57 (2016) 2269–2282, https://doi.org/10.1093/pcp/pcw143.

[24] A. Santana-Sánchez, F. Lynch, S. Sirin, Y. Allahverdiyeva, Nordic cyanobacterial and algal lipids: triacylglycerol accumulation, chemotaxonomy and bioindustrial potential, Physiol. Plant. 173 (2021) 591–602, https://doi.org/10.1111/ppl.13443.

[25] S.Van Wychen, K. Ramirez, L.M.L. Laurens, Determination of Total Lipids as Fatty Acid Methyl Esters (FAME) by In Situ Transesterification: Laboratory Analytical Procedure (LAP), 2016, https://doi.org/10.2172/1118085.

[26] R.M. González-Balderas, M. Felix, C. Bengoechea, M.T. Orta Ledesma, A. Guerrero, S.B. Velasquez-Orta, Development of composites based on residual microalgae biomass cultivated in wastewater, Eur. Polym. J. 160 (2021), 110766, https://doi.org/10.1016/j.eurpolymj.2021.110766.

[27] Y. Tejido-Nuñez, E. Aymerich, L. Sancho, D. Refardt, Treatment of aquaculture effluent with Chlorella vulgaris and Tetradesmus obliquus: the effect of pretreatment on microalgae growth and nutrient removal efficiency, Ecol. Eng. 136 (2019) 1–9, https://doi.org/10.1016/j.ecoleng.2019.05.021.

[28] I.A. Perera, S. Abinandan, L. Panneerselvan, S.R. Subashchandrabose, K. Venkateswarlu, R. Naidu, M. Megharaj, Co-culturing of microalgae and bacteria in real wastewaters alters indigenous bacterial communities enhancing effluent bioremediation, Algal Res. 64 (2022), 102705, https://doi.org/10.1016/j.algal.2022.102705.

[29] L. Rugnini, N.T.W. Ellwood, G. Costa, A. Falsetti, R. Congestri, L. Bruno, Scaling-up of wastewater bioremediation by Tetradesmus obliquus, sequential bio-treatments of nutrients and metals, Ecotoxicol. Environ. Saf. 172 (2019) 59–64, https://doi.org/10.1016/j.ecoenv.2019.01.059.

[30] Y. Su, Revisiting carbon, nitrogen, and phosphorus metabolisms in microalgae for wastewater treatment, Sci. Total Environ. 762 (2021), 144590, https://doi.org/10.1016/j.scitotenv.2020.144590.

[31] S. Ma, Y. Yu, H. Cui, J. Li, Y. Feng, Utilization of domestic wastewater as a water source of Tetradesmus obliquus PF3 for the biological removal of nitric oxide, Environ. Pollut. 262 (2020), 114243, https://doi.org/10.1016/j.envpol.2020.114243.

[32] S. Buono, A. Colucci, A. Angelini, A.L. Langellotti, M. Massa, A. Martello, V. Fogliano, A. Dibenedetto, Productivity and biochemical composition of Tetradesmus obliquus and Phaeodactylum tricornutum: effects of different cultivation approaches, J. Appl. Phycol. 28 (2016) 3179–3192, https://doi.org/10.1007/s10811-016-0876-6.

[33] B. Porto, A.L. Gonçalves, A.F. Esteves, S.M.A.G.U. de Souza, A.A.U. de Souza, V.J. P. Vilar, J.C.M. Pires, Assessing the potential of microalgae for nutrients removal from a landfill leachate using an innovative tubular photobioreactor, Chem. Eng. J. 413 (2021), 127546, https://doi.org/10.1016/j.cej.2020.127546.

[34] L. Francke, S. Löhn, P. Weiderer, A. Kosheleva, N. Wieczorek, K. Kuchta, A novel tubular photobioreactor immersed in open waters for passive temperature control and operated with the microalga Tetradesmus obliquus, Algal Res. 67 (2022), 102832, https://doi.org/10.1016/j.algal.2022.102832.

[35] V.D. Gonçalves, M.R. Fagundes-Klen, D.E.G. Trigueros, A.R. Schuelter, A. D. Kroumov, A.N. Módenes, Combination of light emitting diodes (LEDs) for photostimulation of carotenoids and chlorophylls synthesis in Tetradesmus sp, AlgalRes. 43 (2019), 101649, https://doi.org/10.1016/j.algal.2019.101649.

[36] A.F. Esteves, O.S.G.P. Soares, V.J.P. Vilar, J.C.M. Pires, A.L. Gonçalves, The effect of light wavelength on CO2 capture,biomass production and nutrient uptake by green microalgae: a step forward on process integration and optimisation, Energies 13 (2020) 333, https://doi.org/10.3390/en13020333.

[37] F.Md. Yusoff, N. Nagao, Y. Imaizumi, T. Toda, Bioreactor for microalgal cultivation systems: strategy and development, in: A.A. Rastegari, A.N. Yadav, A. Gupta (Eds.), Prospects of Renewable Bioprocessing in Future Energy Systems, Springer International Publishing, Cham, 2019, pp. 117–159, https://doi.org/10.1007/978-3-030-14463-0_4.

[38] A. Richmond, Biological principles of mass cultivation of photoautotrophic microalgae, in: A. Richmond, Q. Hu (Eds.), Handbook of Microalgal Culture, John Wiley & Sons Ltd, Oxford, UK, 2013, pp. 169–204, https://doi.org/10.1002/9781118567166.ch11.

[39] M. Carneiro, I.B. Maia, P. Cunha, I. Guerra, T. Magina, T. Santos, P.S.C. Schulze, H. Pereira, F.X. Malcata, J. Navalho, J. Silva, A. Otero, J. Varela, Effects of LED lighting on nannochloropsis oceanica grown in outdoor raceway ponds, Algal Res. 64 (2022), 102685, https://doi.org/10.1016/j.algal.2022.102685.

[40] P.S.C. Schulze, H.G.C. Pereira, T.F.C. Santos, L. Schueler, R. Guerra, L.A. Barreira, J.A. Perales, J.C.S. Varela, Effect of light quality supplied by light emitting diodes (LEDs) on growth and biochemical profiles of Nannochloropsis oculata and Tetraselmis chuii, AlgalRes. 16 (2016) 387–398, https://doi.org/10.1016/j.algal.2016.03.034.

[41] M. Arif, Y. Li, M.M. El-Dalatony, C. Zhang, X. Li, E.-S. Salama, A complete characterization of microalgal biomass through FTIR/TGA/CHNS analysis: an approach for biofuel generation and nutrients removal, Renew. Energy 163 (2021) 1973–1982, https://doi.org/10.1016/j.renene.2020.10.066.

[42] R. Delgado, M. dos S. Guarieiro, P.W. Antunes, S.T. Cassini, H.M. Terreros, V. de O. Fernandes, Effect of nitrogen limitation on growth, biochemical composition, and cell ultrastructure of the microalga Picocystis salinarum, J. Appl. Phycol. 33 (2021) 2083–2092, https://doi.org/10.1007/s10811-021-02462-8.

[43] H.M. Amaro, F. Pagels, I.C. Azevedo, J. Azevedo, I. Sousa Pinto, F.X. Malcata, A. C. Guedes, Light-emitting diodes—a plus on microalgae biomass and high-value metabolite production, J. Appl. Phycol. 32 (2020) 3605–3618, https://doi.org/10.1007/s10811-020-02212-2.

[44] R. Admirasari, S. Hindersin, K. von Schwartzenberg, D. Hanelt, Nutritive capability of anaerobically digested black water increases productivity of Tetradesmus obliquus: domestic wastewater as an alternative nutrient resource, Bioresour. Technol.Rep. 17 (2022), 100905, https://doi.org/10.1016/j.biteb.2021.100905.

[45] N. Singh, K. Roy, A. Goyal, V.S. Moholkar, Investigations in ultrasonic enhancement of β-carotene production by isolated microalgal strain Tetradesmus obliquus SGM19, Ultrason. Sonochem. (2019), https://doi.org/10.1016/j.ultsonch.2019.104697.

[46] H. Islami, R. Assareh, Effect of different iron concentrations on growth, lipid accumulation, and fatty acid profile for biodiesel production from Tetradesmus obliquus, J. Appl. Phycol. 31 (2019) 3421–3432, https://doi.org/10.1007/s10811-019-01843-4.

[47] I. Umetani, E. Janka, M. Sposób, C.J. Hulatt, S. Kleiven, R. Bakke, Bicarbonate for microalgae cultivation: a case study in a chlorophyte,Tetradesmus wisconsinensis isolated from a Norwegian lake, J. Appl. Phycol. 33 (2021) 1341–1352, https://doi.org/10.1007/s10811-021-02420-4.

[48] D. Martins, L. Custódio, L. Barreira, H. Pereira, R. Ben-Hamadou, J. Varela, K. Abu-Salah, Alternative sources of n-3 long-chain polyunsaturated fatty acids in marine microalgae, Mar.Drugs 11 (2013) 2259–2281, https://doi.org/10.3390/md11072259.

[49] A. Santin, M.T. Russo, M.I. Ferrante, S. Balzano, I. Orefice, A. Sardo, Highly valuable polyunsaturated fatty acids from microalgae: strategies to improve their yields and their potential exploitation in aquaculture, Molecules 26 (2021) 7697, https://doi.org/10.3390/molecules26247697.

[50] M. Roy, S. Bera, K. Mohanty, Nutrient starvation-induced oxidative stress-mediated lipid accumulation in Tetradesmus obliquus KMC24, J. Appl. Phycol. 33 (2021) 3617–3635, https://doi.org/10.1007/s10811-021-02614-w.

[51] I.B. Maia, M. Carneiro, T. Magina, F.X. Malcata, A. Otero, J. Navalho, J. Varela, H. Pereira, Diel biochemical and photosynthetic monitorization of Skeletonema costatum and Phaeodactylum tricornutum grown in outdoor pilot-scale flat panel photobioreactors, J. Biotechnol. 343 (2022) 110–119, https://doi.org/10.1016/j.jbiotec.2021.11.008.

[52] D.A. Refaay, E.M. El-Marzoki, M.I. Abdel-Hamid, S.A. Haroun, Effect of foliar application with Chlorella vulgaris,Tetradesmus dimorphus, and Arthrospira platensis as biostimulants for common bean, J. Appl. Phycol. 33 (2021) 3807–3815, https://doi.org/10.1007/s10811-021-02584-z.

[53] R. Araújo, F. Vázquez Calderón, J. Sánchez López, I.C. Azevedo, A. Bruhn, S. Fluch, M. Garcia Tasende, F. Ghaderiardakani, T. Ilmjärv, M. Laurans, M. Mac Monagail, S. Mangini, C. Peteiro, C. Rebours, T. Stefansson, J. Ullmann, Current status of the algae production industry in Europe: an emerging sector of the blue bioeconomy, Front. Mar. Sci. 7 (2021), 626389, https://doi.org/10.3389/fmars.2020.626389.

[54] European Parliament , Council of the European Union, Regulation (EU) 2019/1009 of the European Parliament and of the Council of 5 June 2019 laying down rules on the making available on the market of EU fertilising products, n.d.